Pal, 1977), $\Delta T \simeq 15$ K (Chevrier & Saint-James, 1990)]. Another important effect of the deuteration is the temperature width of hysteresis: 3·6 K for a 67 (1)% deuteration compared with 10–30 K for $MnSiF_6.6H_2O$.

Concluding remarks

From Table 1 it can be seen that the atomic positions are perfectly determined in the average structure (space group $R\bar{3}m$). Therefore the bond distances and the angles between atoms are already well known with this approximation. The 'orientational' antiphase model explains the unusual features of the structure (when the space group $P\bar{3}m1$ with an R factor of $R(F) = 0{\cdot}41$ cannot be used), *i.e.* the existence of superlattice reflections and statistical mirrors.

We now have three correlated models to describe the structure of the M fluosilicates (M = Mg, Mn, Fe). In going from Mg^{2+} to Fe^{2+}, the two ordered domains become slightly more complex. Studies on $Mg_{1-x}Fe_xSiF_6.6D_2O$ are now in progress in order to understand this evolution.

I am very grateful to R. Saint-James for preparation of the crystals.

References

BUSING, W. R., MARTIN, K. O. & LEVY, A. (1977). *XFLS*. Oak Ridge National Laboratory, Tennessee, USA.

CHEVRIER, G., HARDY, A. & JEHANNO, G. (1981). *Acta Cryst.* A**37**, 578–584.

CHEVRIER, G. & JEHANNO, G. (1979). *Acta Cryst.* A**35**, 912–916.

CHEVRIER, G. & SAINT-JAMES, R. (1990). *Acta Cryst.* C**46**, 186–189.

GHOSH, B., CHATTERJEE, N., DAS, A. N., DUTTA ROY, S. K. & PAL, A. (1977). *J. Phys. C*, **10**, L527–L529.

HAMILTON, W. C. (1962). *Acta Cryst.* **15**, 353–360.

JEHANNO, G. & VARRET, F. (1975). *Acta Cryst.* A**31**, 857–858.

KODERA, E., TORRI, A., OSAKI, A. & WATANABE, T. (1972). *J. Phys. Soc. Jpn*, **32**, 863–863.

RAY, S., ZALKIN, A. & TEMPLETON, D. (1973). *Acta Cryst.* B**29**, 2741–2747.

SKJAEVELAND, S. M. & SVARE, I. (1974). *Phys. Scr.* **10**, 273–276.

SYOYAMA, S. & OSAKI, K. (1972). *Acta Cryst.* B**28**, 2626–2627.

TSUJIKAWA, I. & COUTURE, L. (1955). *J. Phys. Radium*, **16**, 430–431.

WEIR, R. D., HALSTEAD, K. E. & STAVELEY, L. A. K. (1985). *J. Chem. Soc. Faraday Trans.* 2, **81**, 189–197.

ZACHARIASEN, W. H. (1967). *Acta Cryst.* **23**, 558–564.

Acta Cryst. (1991). B**47**, 228–234

Structures and Phase Transition in the Ferroelectric Crystal of Pentakis-(methylammonium) Undecachlorodibismuthate(III): $[NH_3(CH_3)]_5Bi_2Cl_{11}$

BY JACQUES LEFEBVRE AND PHILIPPE CARPENTIER

Laboratoire de Dynamique des Cristaux Moléculaires, UA 801, *UFR de Physique, Université de Lille* I, 59655 *Villeneuve d'Ascq CEDEX, France*

AND RYSZARD JAKUBAS

Institute of Chemistry, University of Wroclaw, 50 383 *Wroclaw, Poland*

(*Received* 12 *February* 1990; *accepted* 17 *October* 1990)

Abstract

$[NH_3(CH_3)]_5Bi_2Cl_{11}$, $M_r = 968{\cdot}3$; for $T = 294$ K, orthorhombic, $Pca2_1$, $a = 12{\cdot}924$ (2), $b = 14{\cdot}034$ (2), $c = 15{\cdot}364$ (2) Å, $V = 2786{\cdot}6$ (6) Å^3, $Z = 4$, $D_x = 2{\cdot}31$ g cm^{-3}, $R = 0{\cdot}032$ ($wR = 0{\cdot}033$) for 2197 unique reflections; for $T = 349$ K, orthorhombic, $Pcab$, $a = 13{\cdot}003$ (2), $b = 14{\cdot}038$ (3), $c = 15{\cdot}450$ (2) Å, $V = 2820{\cdot}1$ (7) Å^3, $Z = 4$, $D_x = 2{\cdot}28$ g cm^{-3}, $R = 0{\cdot}044$ ($wR = 0{\cdot}037$) for 1219 unique reflections. In the high-temperature phase ($T = 349$ K), $Bi_2Cl_{11}^{5-}$ anions are centrosymmetric bioctahedra and three of the five methylammonium cations are disordered. In the ferroelectric phase ($T = 294$ K), Bi_2Cl_{11} bioctahedra are severely distorted and two of the methylammonium cations are still disordered. The packing is strengthened by N—H···Cl hydrogen bonds between anions and cations. Ordering of the methylammonium cations in the ferroelectric phase leads to new hydrogen-bond formation which is responsible for the high dipolar properties of this compound.

Introduction

Alkylammonium halogenoantimonate(III) and bismuthate(III) salts show a number of interesting properties arising from the possibility of rotational motion of the cations. Most of these compounds display a sequence of phase transitions and some

0108-7681/91/020228-07$03.00

show an important polar character (Jakubas & Sobczyk, 1990). A new member of this family, pentakis(methylammonium) undecachlorodibismuthate(III), $[NH_3(CH_3)]_5Bi_2Cl_{11}$ (hereafter abbreviated to PMACB), has recently been synthesized by Jakubas (1989). From dielectric permittivity measurements and calorimetric studies, it is found that as the temperature is decreased, there is a para–ferroelectric phase transition at $T_{C1} = 307$ K. The temperature dependence of the spontaneous polarization is typical of a second-order phase transition. In particular, the dielectric constant along the polar c axis has a value of the order of 5×10^3 at T_{C1}. In the low-temperature range, a second continuous phase transition appears at $T_{C2} \simeq 160$ K (Jakubas, Sobczyk & Lefebvre, 1989). Pyroelectric studies revealed the low-temperature transition for PMACB (Mroz & Jakubas, 1990) to be of the ferro–ferroelectric type.

The bromine analogue, $[NH_3(CH_3)]_5Bi_2Br_{11}$, exhibits the same para–ferroelectric phase transition as PMACB (Jakubas & Sobczyk, 1989), and recently its structure has been solved in the ferroelectric phase (Matuszewski, Jakubas, Sobczyk & Głowiak, 1990). Some methylammonium cations display a partial disorder which could be the origin of the high value of the dielectric constant.

In this paper, the structures of the high-temperature phase ($T = 349$ K) and the ferroelectric phase ($T = 294$ K) of PMACB have been solved. The mechanism of the phase transition is given and related to the important polar character of this compound.

Experimental

PMACB was prepared by reaction of $(BiO)_2CO_3$ with CH_3NH_3Cl in concentrated HCl. It was purified by repeated crystallization. Single crystals were grown from dilute HCl. The composition of the compound was determined by elemental analysis.

Because of the high absorption of PMACB, the single crystals used for X-ray diffraction were of a spherical shape, achieved by polishing samples using a specially designed device. Two different single crystals were used for data collection at 294 and 349 K (diameters 0·21 and 0·19 mm, respectively).

Intensity measurements were performed using an Enraf–Nonius CAD-4 X-ray automatic diffractometer. The incident X-ray beam [λ(Mo $K\alpha$) = 0·7107 Å] was monochromatized with a pyrolitic graphite crystal. For measurements at 349 K, a device with a controlled gas stream was used (Tuinstra & Fraase Storm, 1978). The temperature stability was better than 1 K. Unit-cell dimensions at the two temperatures were refined from the position of 25 reflections in the range $15 < 2\theta < 22°$. ω–2θ The scan mode was used with scan width $\Delta\omega = (0{\cdot}50 + 0{\cdot}34\tan\theta)°$ and in the range $2 < \omega < 30°$ ($0{\cdot}05 < \sin\omega/\lambda < 0{\cdot}70$ Å^{-1}). The scan speed was adjusted to obtain $\sigma(I)/I = 0{\cdot}03$ with a maximum counting time of 3 min. Three orientation control reflections were checked every 100 reflections. Intensities of three standard reflections were measured every 2 h at room temperature and at 1 h intervals at 349 K. A decay of 7% and 3% was observed at room temperature and 349 K, respectively. Corrections were applied using the *SDP* program (B. A. Frenz & Associates Inc., 1985).

Table 1. *Data collection and refinement parameters*

	High-temperature phase (349 K)	Ferroelectric phase (294 K)
Space group	*Pcab*	*Pca2*$_1$
Z	4	4
a (Å)	13·003 (2)	12·924 (2)
b (Å)	14·038 (3)	14·034 (2)
c (Å)	15·450 (2)	15·364 (2)
V (Å^3)	2820·1 (7)	2786·6 (6)
D_x (g cm^{-3})	2·28	2·31
No. of measured reflections	5000	8151
No. of observed reflections $[I > \sigma(I)]$	1219	2197
μ (cm^{-1})	134·8	136·6
μr	1·3	1·4
Transmission factor (maximum)	0·190	0·171
Transmission factor (minimum)	0·165	0·141
No. of parameters	114	205
R	0·044	0·032
wR*	0·037	0·033
h,k,l range	$0 \le h \le 18$	$-18 \le h \le 18$
	$0 \le k \le 19$	$0 \le k \le 19$
	$0 \le l \le 21$	$0 \le l \le 18$
$\Delta\rho$ (e Å^{-3})	1·5	1·2
	−1·0	−0·9
S	5·2	3·0

* Weighting scheme: $w = [\sigma^2(F) + 10^{-4}F^2]^{-1}$.

Crystal data and details of the structure refinement are reported in Table 1. The intensity data were corrected for Lorentz–polarization factors. A spherical absorption correction was applied (*SDP* program). In order to check the sphericity of the single crystal, equivalent h,k,l and $\bar{h},k,l$ reflections were systematically measured at room temperature. The agreement factor, when averaged values were calculated, was 0·026 for the structure factors of 'observed' reflections. Scattering factors of neutral atoms were approximated using the analytical expression, with a_i, b_i and c_i coefficients, from *International Tables for X-ray Crystallography* (1974, Vol. IV). Anomalous-dispersion effects for heavy atoms were taken into account (Cromer & Liberman, 1970). The maximum shift in the last cycle was less than $0{\cdot}1\sigma$.

At room temperature the unit cell is orthorhombic. From the density, $D_m = 2{\cdot}31$ g cm^{-3}, measured by a flotation technique, it can be deduced that there are four molecules of PMACB per unit cell. Systematic absences of $0kl$ reflections for l odd and $h0l$ reflections for h odd lead to *Pcam* or *Pca*2$_1$ as possible space groups. From dielectric measurements it is known that PMACB is polar at room tempera-

Table 2. *Positional parameters* ($\times 10^4$) *and equivalent isotropic temperature factors* ($Å^2 \times 10^3$)

$U_{eq} = \frac{1}{3}\text{trace}(U)$.

	x	y	z	U_{eq}
349 K				
Bi	−1622 (1)	822 (1)	1091 (1)	47 (1)
Cl(1)	0	0	0	77 (12)
Cl(2)	−575 (4)	2487 (4)	1144 (3)	72 (8)
Cl(3)	−2637 (4)	−858 (4)	1046 (3)	81 (8)
Cl(4)	−2958 (4)	1522 (4)	2122 (3)	104 (8)
Cl(5)	−558 (4)	194 (5)	2478 (4)	97 (9)
Cl(6)	−2701 (5)	1433 (4)	−275 (3)	102 (9)
N(1)	−857 (18)	2679 (16)	3222 (11)	125 (39)
N(2)	1762 (23)	1466 (19)	932 (21)	75 (48)
N(2)′	1850 (38)	180 (42)	1609 (31)	92 (91)
N(3)	79 (48)	4533 (41)	403 (50)	164 (31)
C(1)	88 (19)	2629 (23)	3671 (14)	107 (48)
C(2)	1930 (49)	801 (46)	1627 (30)	111 (19)
C(2)′	2202 (44)	1045 (39)	1317 (39)	60 (20)
C(3)	124 (42)	5172 (46)	−324 (37)	76 (18)
294 K				
Bi(1)	−1696 (1)	826 (1)	1010	41 (1)
Bi(2)	1570 (1)	−811 (1)	−1179 (1)	44 (1)
Cl(1)	−83 (4)	40 (6)	21 (5)	66 (6)
Cl(12)	−674 (3)	2521 (3)	1096 (3)	58 (5)
Cl(13)	−2701 (4)	−836 (3)	1157 (4)	71 (7)
Cl(14)	−3007 (4)	1554 (4)	2147 (3)	83 (6)
Cl(15)	−610 (4)	291 (4)	2490 (4)	86 (8)
Cl(16)	−2889 (4)	1373 (4)	−281 (3)	82 (7)
Cl(22)	461 (4)	−2404 (4)	−1227 (4)	74 (7)
Cl(23)	2638 (4)	886 (3)	−937 (4)	67 (6)
Cl(24)	2944 (4)	−1488 (4)	−2109 (4)	95 (7)
Cl(25)	541 (4)	−97 (4)	−2502 (4)	84 (7)
Cl(26)	2534 (4)	−1479 (4)	294 (4)	90 (7)
N(11)	−907 (12)	2713 (11)	3200 (11)	83 (25)
N(21)	−884 (16)	7605 (17)	1692 (18)	113 (36)
N(12)	1737 (14)	1506 (15)	893 (14)	82 (7)
N(12)′	1810 (57)	192 (57)	1763 (52)	50 (24)
N(22)	1792 (32)	6445 (29)	3958 (23)	58 (13)
N(22)′	1778 (23)	5249 (26)	3459 (18)	64 (9)
N(3)	−136 (13)	4719 (20)	399 (17)	142 (39)
C(11)	120 (16)	2572 (18)	3690 (13)	104 (33)
C(21)	88 (15)	7774 (20)	1350 (15)	165 (44)
C(12)	1984 (20)	823 (21)	1661 (18)	85 (7)
C(12)′	1348 (95)	1127 (65)	1954 (85)	78 (41)
C(22)	2031 (48)	5697 (50)	3426 (32)	73 (14)
C(22)′	2212 (35)	6116 (32)	3805 (30)	72 (11)
C(3)	−20 (18)	5390 (18)	−232 (21)	88 (38)

Table 3. *Bond lengths* (Å) *and angles* (°) *in PMACB, in the high-temperature phase* ($T = 349$ K) *and in the ferroelectric phase* ($T = 294$ K)

	High-temperature phase	Ferroelectric phase $i = 1$	Ferroelectric phase $i = 2$	Relative variation (%)*
Bi(i)—Cl(1)	2·937 (1)	2·807 (7)	3·063 (7)	8·7
Bi(i)—Cl(i2)	2·706 (5)	2·724 (5)	2·657 (5)	2·5
Bi(i)—Cl(i3)	2·704 (5)	2·679 (5)	2·777 (4)	3·6
Bi(i)—Cl(i4)	2·553 (5)	2·639 (5)	2·469 (5)	6·6
Bi(i)—Cl(i5)	2·699 (5)	2·776 (6)	2·628 (6)	5·5
Bi(i)—Cl(i6)	2·675 (5)	2·627 (5)	2·748 (6)	4·5
N(i1)—C(i1)	1·41 (3)	1·54 (3)	1·38 (3)	
N(i2)—C(i2)	1·44 (4)	1·55 (4)	1·37 (8)	
N(i2)′—C(i2)′	1·37 (5)	1·47 (13)	1·44 (6)	
N(3)—C(3)	1·44 (5)	1·36 (4)		
Cl(1)—Bi(i)—Cl(i2)	89·7 (1)	90·5 (2)	88·2 (2)	
Cl(1)—Bi(i)—Cl(i3)	89·6 (1)	93·6 (2)	86·1 (2)	
Cl(1)—Bi(i)—Cl(i4)	176·4 (1)	171·0 (2)	178·2 (2)	
Cl(1)—Bi(i)—Cl(i5)	87·6 (1)	87·8 (2)	87·9 (2)	
Cl(1)—Bi(i)—Cl(i6)	92·8 (1)	98·2 (2)	87·4 (2)	
Cl(i2)—Bi(i)—Cl(i3)	179·0 (2)	172·4 (1)	173·4 (2)	
Cl(i2)—Bi(i)—Cl(i4)	89·5 (2)	86·6 (1)	92·9 (2)	
Cl(i2)—Bi(i)—Cl(i5)	90·0 (2)	87·2 (2)	91·5 (2)	
Cl(i2)—Bi(i)—Cl(i6)	90·6 (2)	93·8 (2)	88·9 (2)	
Cl(i3)—Bi(i)—Cl(i4)	91·1 (2)	88·3 (2)	92·9 (2)	
Cl(i3)—Bi(i)—Cl(i5)	89·2 (2)	86·6 (2)	91·6 (2)	
Cl(i3)—Bi(i)—Cl(i6)	90·2 (2)	91·9 (2)	87·5 (2)	
Cl(i4)—Bi(i)—Cl(i5)	88·8 (2)	83·5 (2)	93·6 (2)	
Cl(i4)—Bi(i)—Cl(i6)	90·7 (2)	90·6 (2)	91·1 (2)	
Cl(i5)—Bi(i)—Cl(i6)	179·2 (2)	173·9 (2)	175·3 (2)	
Bi(1)—Cl(1)—Bi(2)	180·0	175·7 (3)		

* The relative variation of bond lengths is given by $r = [2\,d_{Bi(1)\cdots Cl(1i)} - d_{Bi(2)\cdots Cl(2i)}|]/[d_{Bi(1)\cdots Cl(1i)} + d_{Bi(2)\cdots Cl(2i)}]$.

ture (Jakubas, Sobczyk & Lefebvre, 1989) and hence its space group is $Pca2_1$. In the high-temperature phase, the unit cell is also orthorhombic, with almost the same lattice parameters as at room temperature (except for thermal expansion), and $Z = 4$. The two previous systematic absences are also present in this phase and a third one appears: $hk0$ for k odd, leading to the centrosymmetric space group *Pcab*. [In order to have consistent atomic coordinates between the two phases, the symmetry operations of $Pca2_1$ differ somewhat from those given in *International Tables for X-ray Crystallography* (1952, Vol. 1). They are: x, y, z; $-x, \frac{1}{2}-y, \frac{1}{2}+z$; $\frac{1}{2}-x, y, \frac{1}{2}+z$; $\frac{1}{2}+x, \frac{1}{2}-y, z$.]

All calculations were performed using *SHELX*76 (Sheldrick, 1976). For the room-temperature structure, Patterson synthesis allows the position of the Bi atoms to be determined. From successive difference syntheses, all Cl, and then C and N, atoms can be located. In order to determine the H-atom positions, a new difference synthesis was calculated which produced some peaks near two of the five methylammonium cations. However, these peaks do not correspond to H atoms but to orientational disorder of two of the methylammonium cations. The z coordinate of one of the Bi atoms is fixed. All ordered atoms have been refined using anisotropic temperature factors; for disordered atoms, thermal motions were assumed to be isotropic.

In order to solve the structure of the high-temperature phase, the central Cl atom is defined as being located at the centre of inversion and the starting coordinates for all other heavy atoms are those obtained at room temperature; C and N atoms are removed in the first instance. Because the unit cell contains 20 methylammonium cations and the degree of symmetry of the space group is eight, four methylammonium cations must be disordered with an occupancy probability of 0·5. A difference synthesis allowed all the C and N atoms of the five methylammonium cations to be located, three of which are found to be disordered: the two which were already disordered in the ferroelectric phase (now related to each other by the inversion centre) and a third for which the disorder can be deduced by symmetry arguments. Attempts were made to refine all atoms using anisotropic temperature factors. However, for most of the disordered atoms, strong correlations between variable parameters meant that finally four atoms had to be refined using isotropic temperature factors [C(20, C(2′), N(3) and C(3)].

Results and discussion

Final atomic coordinates and equivalent temperature factors for the two phases are presented in Table 2.* Bond lengths and bond angles are given in Table 3. A drawing of the $Bi_2Cl_{11}^{5-}$ anion in the ferroelectric phase, using *ORTEP*II (Johnson, 1976), is presented in Fig. 1. Numbering of the Bi and Cl atoms is shown in this figure. Examples of projections of the unit-cell contents along *a* and *b* for the high-temperature phase are given in Fig. 2. The same projections for the ferroelectric phase are presented in Fig. 3. Numbering of atoms for the methylammonium cations is as follows: an atom of the high-temperature phase, called *A(j)*, generates two atoms in the room-temperature phase *A*(1*j*) and *A*(2*j*). For disordered methylammonium cations the two equilibrium positions are labelled by primed and unprimed atoms with the same numbering.

For the two phases the final difference synthesis exhibits important peaks and holes in the residual electron density. These peaks and holes are all located around the Bi atoms where the assumption of spherically symmetric electron density seems to be incorrect. For example, all peaks greater than 0·75 e $Å^{-3}$ are located at approximately 1 Å from the Bi atoms. As a consequence, the positions of the H atoms cannot be found and the ionic character of the Bi and Cl atoms cannot be determined.

As shown in Fig. 1, the $Bi_2Cl_{11}^{5-}$ anion forms a bioctahedron with a common Cl atom [Cl(1)]. In the high-temperature phase this bioctahedron is centrosymmetric with Cl(1) located at the inversion centre. As for the Bi—Cl bonds, the bridging Bi—Cl(1) bond is longer (2·937 Å) and the Bi—Cl(4) bond shorter (2·553 Å) [along the direction of the Bi—Cl(1) bond] than the other four terminal bonds (average value 2·70 Å). Most of the bond angles have values near 90 or 180°, as expected for a perfect octahedron, and all atoms of this anion lie in two perpendicular planes [only Cl(4) is 0·12 Å out of one of the two planes]. By way of contrast, at room temperature, the $Bi_2Cl_{11}^{5-}$ anion undergoes an important distortion. Firstly, the distance between the centre of mass of the ion and the central Cl(1) atom

* Lists of structure factors and anisotropic thermal parameters have been deposited with the British Library Document Supply Centre as Supplementary Publication No. SUP 53601 (27 pp.). Copies may be obtained through The Technical Editor, International Union of Crystallography, 5 Abbey Square, Chester CH1 2HU, England.

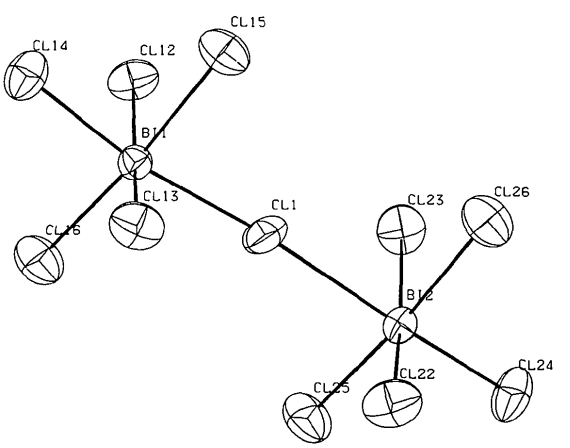

Fig. 1. *ORTEP*II view of the Bi_2Cl_{11} bioctaedra in the ferroelectric phase ($T = 294$ K).

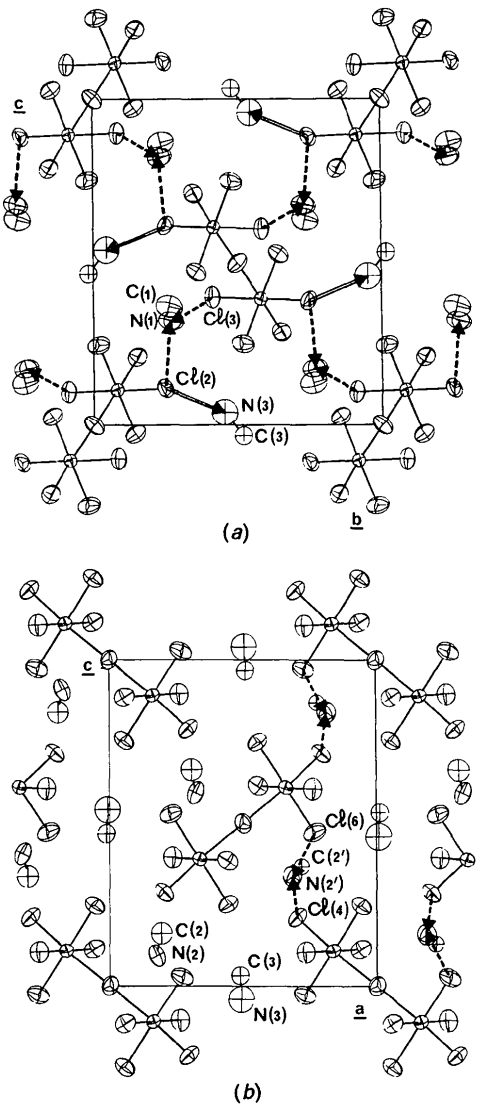

Fig. 2. Projection of the unit-cell contents in the high-temperature phase ($T = 349$ K): (*a*) projection along *a* and (*b*) projection along *b*. The dotted lines represent N···Cl hydrogen bonds from N(1) or N(2), double lines represent N···Cl hydrogen bonds from N(3). Only atoms near the planes $x = 0$ [for (*a*)] and $y = 0$ [for (*b*)] are drawn.

is 0·089 Å, with an important component along the polar *c* axis. For equivalent Bi—Cl bonds in the high-temperature phase, relative variations at room temperature range from 2·5 to 8·8% (Table 3); the maximum value of these variations corresponds to the bridging Bi—Cl(1) bond. The bond angles also deviate from 90 and 180°: from 83·5 to 98·2° on the one hand and from 171 to 178·2° on the other. In particular, the value of the central Bi(1)—Cl(1)—Bi(2) angle is 175·7°. An explanation of these distortions is given below.

In the high-temperature phase, two methylammonium cations of the PMACB molecule are ordered [those generated by N(1)—C(1)] and the other three disordered [generated by N(2)—C(2) and N(3)—C(3)]. This type of disorder has been suggested in the case of the bromine analogue $[NH_3(CH_3)]_5Bi_2Br_{11}$ (Matuszewski *et al.*, 1990) at room temperature, but it could not be characterized by the authors. This type of disorder consists of two equilibrium positions for each methylammonium cation between which the cation can jump. Table 4 gives the characteristics of reorientational motions for each disordered methylammonium cation. The translation calculated in this table is the distance between the centres of the C—N bonds corresponding to the two equilibrium positions.

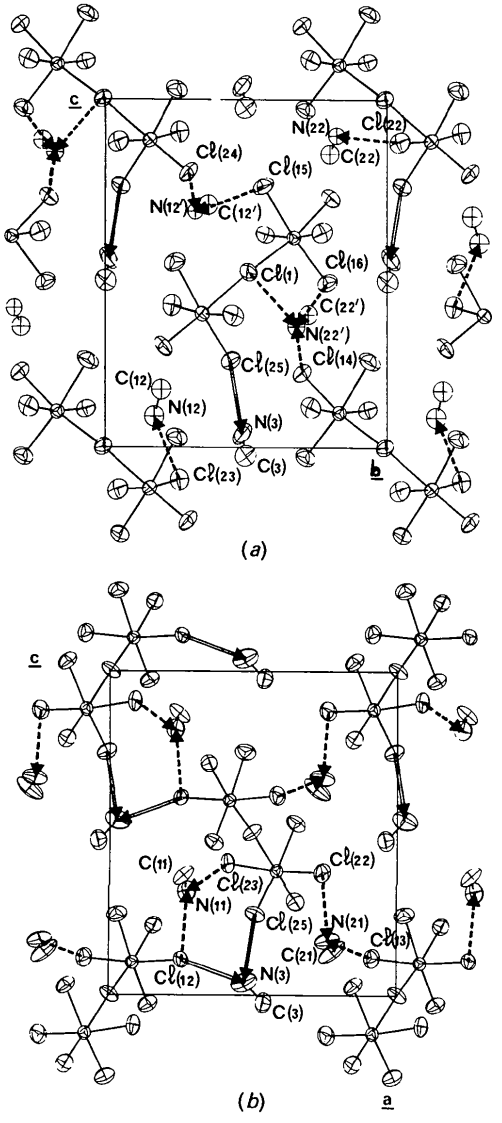

Fig. 3. (*a*), (*b*) Projection of the unit-cell contents in the ferroelectric phase (T = 294 K) (same caption as for Fig. 2).

Table 4. *Characterization of the disorder of methylammonium cations*

	Occupancy probability of unprimed atoms	Reorientational process Rotation (°)	Translation (Å)
349 K			
Methylammonium (2)	0·60 (5)	140	0·82 (15)
Methylammonium (3)	0·50	180	0·51 (19)
294 K			
Methylammonium (12)	0·84 (3)	119	1·20 (20)
Methylammonium (22)	0·40 (6)	141	0·56 (12)

In the ferroelectric phase, at room temperature, methylammonium (3) becomes ordered. In fact, it is not realistic to think that this cation, which is disordered in the high-temperature phase, suddenly becomes ordered when the transition is crossed, but rather that a progressive ordering becomes established as the temperature decreases. Nevertheless, at 294 K (T_c − 13 K), no significant residual electron density appears in the neighbourhood of this methylammonium cation and for this reason, it has been considered as completely ordered. The two methylammonium cations corresponding to cation (2) of the high-temperature phase are still disordered. The occupancy probability of cation (12) increases with respect to its value at 349 K, whereas it decreases for cation (22). (For the ferroelectric phase, the values of occupancy probabilities given in Table 4 correspond to the equilibrium position with an occupancy probability of 0·60 at high temperature.)

In the two phases the C—N bond lengths vary considerably, ranging from 1·37 to 1·55 Å. For methylammonium cations, the values usually found in the literature for this bond are: 1·56 Å (Schlimper & Ziegler, 1972), 1·47 Å (Khan & Tuck, 1981) and 1·44 Å (Caputo & Willet, 1981). The smaller values obtained in the present work seem to be a consequence of either orientational disorder of the cations or the large vibrational thermal motion. For example, shortening of the C—N bond length of methylammonium (21) is due to this effect.

Packing in the two phases can be summarized in the following way: bioctahedra of $Bi_2Cl_{11}^{5-}$ anions are approximately located at the corner and at the centre of each face of the cell. The methylammonium

Table 5. *Selected* Cl···N *distances* (Å)

349 K

Cl(2)···N(1)	3·24 (3)	Cl(4)···N(2^{iii})	3·10 (9)
Cl(3)···N(1')	3·30 (5)	Cl(6)···N(2^{iii})	3·26 (10)
	Cl(2)···N(3) 3·21 (10)		

Symmetry code: (i) $x, y-\frac{1}{2}, \frac{1}{2}-z$; (ii) $x-\frac{1}{2}, -y, \frac{1}{2}-z$; (iii) $-x, -y, -z$.

249 K

Cl(12)···N(11)	3·26 (3)	Cl(22)···N(21')	3·26 (4)
Cl(23)···N(11')	3·26 (4)	Cl(13)···N(21^{ii})	3·31 (5)
Cl(23)···N(12)	3·17 (4)	Cl(22)···N(22')	3·22 (7)
Cl(14)···N(12^{iii})	3·35 (4)	Cl(24)···N(22^{iv})	3·35 (7)
Cl(24)···N(12')'	2·95 (13)	Cl(14)···N(22^{iii})'	3·25 (6)
Cl(15)···N(12)'	3·32 (11)	Cl(1)···N(22')'	3·27 (6)
		Cl(16)···N(22')'	3·32 (7)
	Cl(25)···N(3') 3·31 (4)		
	Cl(12)···N(3) 3·34 (5)		

Symmetry code: (i) $-x, \frac{1}{2}-y, z-\frac{1}{2}$; (ii) $x, y-1, z$; (iii) $x-\frac{1}{2}, \frac{1}{2}-y, z$; (iv) $\frac{1}{2}-x, y-1, z-\frac{1}{2}$; (iv) $\frac{1}{2}-x, y, z-\frac{1}{2}$.

cations lie between two Bi_2Cl_{11} bioctahedra: for methylammonium (*i*1) they are, approximately, along the (011) and (0$\bar{1}$1) directions, for methylammonium (*i*2) they lie along (101) and ($\bar{1}$01) and, finally, for methylammonium (3) are located in the middle of each edge of the cell. Table 5 gives the Cl···N distances less than 3·35 Å and corresponding to possible hydrogen bonds: a weak N—H···Cl hydrogen bond has a length of the order of 3·22 Å (Pimentel & McClellan, 1960; Schlimper & Ziegler, 1972). In the high-temperature phase, for the ordered methylammonium cation (1), its N atom is involved in two hydrogen bonds with a Cl atom from each of its two nearest neighbour Bi_2Cl_{11} anions (see Fig. 2*a*). In the ferroelectric phase, the interactions are almost the same with the two non-equivalent methylammonium cations (11) and (21) (Fig. 3*a*), these two cations not being involved in the phase-transition mechanism.

The situation is not so clear in the case of methylammonium cations (*i*2), which are disordered in both phases. In the high-temperature phase and for the more-occupied equilibrium position, there is no hydrogen bond; for the other position there are two hydrogen bonds with the nearest neighbour Bi_2Cl_{11} anions (Fig. 2*b*). When the transition takes place, the hydrogen bonds are different for the four possible equilibrium positions. Some new hydrogen bonds appear in this phase, as for example, is the case for Cl(1)···N(22') (Fig. 3*b*). Nevertheless, as these methylammonium cations are disordered in both phases, they cannot be responsible for the phase transition.

Finally, methylammonium (3) is disordered in the high-temperature phase and is involved in the hydrogen bond Cl(2)···N(3). In the ferroelectric phase, this cation becomes ordered and forms the new hydrogen bond Cl(25)···N(3) (Fig. 3). This bond is essentially oriented along *c* and consequently is responsible for the strong polar character of the ferroelectric phase. As mentioned previously, ordering of this methylammonium is not complete when the transition takes place and the probability of finding it in an orientation called 'up' (shown in Fig. 3) is $p(3)$, with $0{\cdot}5 < p(3) < 1$. Likewise, there is a probability $p(3)$ for a similar Cl(25)···N(3) hydrogen bond, and a probability $[1-p(3)]$ for a Cl(15)···N(3) hydrogen bond corresponding to an orientation 'down'. On the other hand, if, in the PMACB unit cell, the contribution to the dipole moment can be reduced by adding this hydrogen bond (contributions from all other hydrogen bonds vanish), the component of the molecular dipole moment along *c*, and consequently, the spontaneous polarization, is proportional to $2p(3)-1$. This spontaneous polarization has been measured by Jakubas, Sobczyk & Lefebvre, (1989) in the transition-temperature region (Fig. 4). The occupancy probability $p(3)$ at 294 K, deduced from this measurement, is 0·89. Therefore, it is not surprising that the 'down' orientation is not observed for this cation.

As stated above, the Bi_2Cl_{11} bioctaedra show significant distortion in the ferroelectric phase. Firstly, it should be noted that the sum of the two Bi(*i*)—Cl(1) bond lengths is constant for both phases: 5·874 (2) Å at 349 K and 5·870 (14) Å at room temperature. Secondly, distortion of the two bridging bonds is due to a displacement of the central Cl(1) atom which is involved in a hydrogen bond only present in the ferroelectric phase. The same conclusion can be drawn concerning Cl(*i*4), Cl(*i*5) and Cl(*i*6), where equivalent atoms have very different neighbourhoods in the ferroelectric phase. By contrast, Cl(*i*2) and Cl(*i*3) are involved in approximately the same hydrogen bonds in both phases and the distortions are smaller.

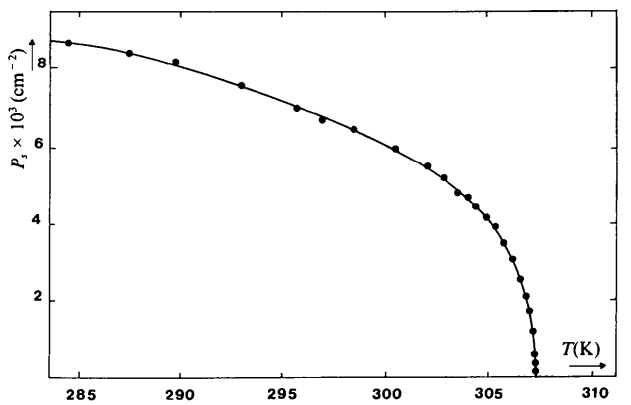

Fig. 4. Spontaneous polarization as a function of temperature.

References

B. A. FRENZ & ASSOCIATES INC. (1985). *SDP Structure Determination Package*. College Station, Texas, USA, and Enraf–Nonius, Delft, The Netherlands.

CAPUTO, R. E. & WILLET, R. D. (1981). *Acta Cryst.* B37, 1616–1617.
CROMER, D. T. & LIBERMAN, D. (1970). *J. Chem. Phys.* **53**, 1891–1898.
JAKUBAS, R. (1989). *Solid State Commun.* **60**, 389–391.
JAKUBAS, R. & SOBCZYK, L. (1989). *Ferroelectrics*, **92**, 365–368.
JAKUBAS, R. & SOBCZYK, L. (1990). *Phase Transitions*, **20**, 163–193.
JAKUBAS, R., SOBCZYK, L. & LEFEBVRE, J. (1989). *Ferroelectrics*, **100**, 143–149.
JOHNSON, C. K. (1976). *ORTEP*II. Report ORNL-5138. Oak Ridge National Laboratory, Tennessee, USA.
KHAN, M. A. & TUCK, D. G. (1981). *Acta Cryst.* B37, 683–685.
MATUSZEWSKI, J., JAKUBAS, R., SOBCZYK, L. & GŁOWIAK, T. (1990). *Acta Cryst.* C46, 1385–1388.
MROZ, J. & JAKUBAS, R. (1990). *Ferroelectric Lett.* **11**, 53–56.
PIMENTEL, G. C. & MCCLELLAN, A. L. (1960). *The Hydrogen Bond*, pp. 290–291. San Francisco: Freeman.
SCHLIMPER, H. U. & ZIEGLER, M. L. (1972). *Z. Naturforsch. Teil B*, **27**, 377–379.
SHELDRICK, G. M. (1976). *SHELX*76. Program for crystal structure determination. Univ. of Cambridge, England.
TUINSTRA, F. & FRAASE STORM, G. M. (1978). *J. Appl. Cryst.* **11**, 257–259.

Acta Cryst. (1991). B47, 234–239

Structures of the 3:1 Adducts of Cadmium(II) Bromide and of Cadmium(II) Chloride with 15-Crown-5 Ether:* Structural Changes Induced by Radiation

BY ALAN HAZELL, RITA GRØNBÆK HAZELL, MONA FRØYDIS HOLM AND LONE KROGH

Institute of Chemistry, Aarhus University, DK-8000 Århus C, Denmark

(*Received* 14 *May* 1990; *accepted* 23 *October* 1990)

Abstract

$3CdBr_2.C_{10}H_{20}O_5$, $M_r = 1036{\cdot}9$, monoclinic, $P2_1/c$, $a = 7{\cdot}535\ (6)$, $b = 14{\cdot}452\ (17)$, $c = 11{\cdot}771\ (12)$ Å, $\beta = 116{\cdot}54\ (2)°$, $V = 1147\ (2)$ Å^3, $Z = 2$, $D_x = 3{\cdot}00$ g cm^{-3}, Mo $K\alpha$, $\lambda = 0{\cdot}71073$ Å, $\mu = 131{\cdot}2$ cm^{-1}, $F(000) = 948$, $T = 295$ K, $R(F) = 0{\cdot}036$ for 1234 reflexions [$I \geq 3\sigma(I)$] and 105 variables. $3CdCl_2.C_{10}H_{20}O_5$, ordered structure, $M_r = 770{\cdot}2$, monoclinic, $P2_1$, $a = 7{\cdot}217\ (1)$, $b = 14{\cdot}235\ (2)$, $c = 11{\cdot}255\ (1)$ Å, $\beta = 115{\cdot}835\ (8)°$, $V = 1040{\cdot}7\ (2)$ Å^3, $Z = 2$, $D_x = 2{\cdot}46$ g cm^{-3}, Mo $K\alpha$, $F(000) = 732$, $T = 295$ K. $3CdCl_2.C_{10}H_{20}O_5$, disordered structure, second data set, $M_r = 770{\cdot}2$, monoclinic, $P2_1/c$, $a = 7{\cdot}231\ (3)$, $b = 14{\cdot}331\ (21)$, $c = 11{\cdot}284\ (7)$ Å, $\beta = 116{\cdot}00\ (2)°$, $V = 1051\ (2)$ Å^3, $Z = 2$, $D_x = 2{\cdot}43$ g cm^{-3}, Mo $K\alpha$, $\mu = 37{\cdot}9$ cm^{-1}, $F(000) = 732$, $T = 295$ K, $R(F) = 0{\cdot}035$ for 2285 reflexions [$I > 3\sigma(I)$] and 105 variables. $3CdCl_2.C_{10}H_{20}O_5$, disordered structure, third data set, $M_r = 770{\cdot}2$, monoclinic, $P2_1/c$, $a = 7{\cdot}236\ (4)$, $b = 14{\cdot}417\ (46)$, $c = 11{\cdot}312\ (13)$ Å, $\beta = 116{\cdot}05\ (5)°$, $V = 1060\ (4)$ Å^3, $Z = 2$, $D_x = 2{\cdot}41$ g cm^{-3}, Mo $K\alpha$, $\mu = 37{\cdot}6$ cm^{-1}, $F(000) = 732$, $T = 295$ K, $R(F) = 0{\cdot}041$ for 2073 reflexions [$I > 3\sigma(I)$] and 105 variables. $3CdCl_2.C_{10}H_{20}O_5$, disordered structure, fourth data set, $M_r = 770{\cdot}2$, monoclinic, $P2_1/c$, $a = 7{\cdot}249\ (1)$, $b = 14{\cdot}521\ (19)$, $c = 11{\cdot}350\ (5)$ Å, $\beta = 116{\cdot}15\ (3)°$, $V = 1072\ (2)$ Å^3, $Z = 2$, $D_x = 2{\cdot}38$ g cm^{-3}, Mo $K\alpha$, $\mu = 37{\cdot}1$ cm^{-1}, $F(000) = 732$, $T = 293$ K, $R(F) = 0{\cdot}054$ for 1862 reflexions [$I > 3\sigma(I)$] and 105 variables. $3CdCl_2.C_{10}H_{20}O_5$, disordered structure, fifth data set, $M_r = 770{\cdot}2$, monoclinic, $P2_1/c$, $a = 7{\cdot}251\ (1)$, $b = 14{\cdot}560\ (19)$, $c = 11{\cdot}360\ (5)$ Å, $\beta = 116{\cdot}19\ (3)°$, $V = 1076\ (2)$ Å^3, $Z = 2$, $D_x = 2{\cdot}38$ g cm^{-3}, Mo $K\alpha$, $\mu = 37{\cdot}0$ cm^{-1}, $F(000) = 732$, $T = 293$ K, $R(F) = 0{\cdot}060$ for 1713 reflexions [$I > 3\sigma(I)$] and 105 variables. For the disordered structures, *i.e.* the bromide and data sets 2–5 for the chloride, the cell dimensions are the mean of those measured before and after the intensity measurements. The compounds are isostructural; both contain trigonal and pentagonal bipyramidally coordinated Cd atoms which are linked by halogen bridges to form sheets perpendicular to *b*. The Cd atom at the centre of the crown ether, which is disordered, is bonded by strong Cd—O bonds [Cd—O 2·22 (2) to 2·38 (2) Å in the bromide and 2·239 (5) to 2·404 (6) Å in the chloride]. The axial Cd—Br bonds [2·812 (3) to 2·878 (2) Å] are longer than the equatorial Cd—Br bonds [2·623 (2) to 2·640 (2) Å]. The axial Cd—Cl bonds range from 2·651 to 2·691 (1) Å and the equatorial Cd—Cl bonds from 2·508 (1) to 2·535 (1) Å. Both compounds suffer radiation damage which results in changes in the cell dimensions during data collection and, for the chloride, a phase transition occurs in which the crown becomes disordered and the space group changes from $P2_1$ to $P2_1/c$.

Introduction

The dihalides of cadmium and mercury form 1:1 complexes with 18-crown-6 ether (18C6) in which the

* 1,4,7,10,13-Pentaoxacyclopentadecane.

0108-7681/91/020234-06$03.00